Time resolved measurements of gratings photo-induced by femtosecond pulses in a lead doped glass

Souad Chouli, Eric Freysz

Time resolved measurements of gratings photo-induced by femtosecond pulses in a lead doped glass

S. Chouli[1,2] and E. Freysz[1,2,*]

[1]*Université de Bordeaux, LOMA, UMR-5798, F-33400 Talence, France*
[2]*CNRS LOMA, UMR-5798, F-33400 Talence, France*
**e.freysz@loma.u-bordeaux1.fr*

Abstract: We report on the formation of gratings photo-induced by femtosecond laser pulses in SF59 glass. Depending on the number of pulses used to excite the sample and the pump power density, transient or permanent gratings are induced. We demonstrate that the grating formation is not instantaneous and is produced by laser-induced defects. This results in a change of both the real and imaginary part of the index of refraction. A simple set-up that records the temporal evolution of both parameters during the laser excitation is also presented. It makes it possible to evaluate the weight of both contributions to the grating diffraction efficiency.

OCIS codes: (140.3390) Laser materials processing; (140.3440) Laser-induced breakdown; (320.7130) Ultrafast processes in condensed matter, including semiconductors; (160.2750) Glass and other amorphous materials; (320.2250) Femtosecond phenomena.

References and links

1. H. Zhang, S. M. Eaton, J. Li, and P. R. Herman, "Femtosecond laser direct writing of multiwavelength Bragg grating waveguides in glass," Opt. Lett. **31**(23), 3495–3497 (2006).
2. H. Zhang, S. M. Eaton, and P. R. Herman, "Single-step writing of Bragg grating waveguides in fused silica with an externally modulated femtosecond fiber laser," Opt. Lett. **32**(17), 2559–2561 (2007).
3. W. Yang, P. G. Kazansky, and Y. P. Svirko, "Non-reciprocal ultrafast laser writing," Nat. Photonics **2**(2), 99–104 (2008).
4. M. Lancry, B. Poumellec, A. Chahid-Erraji, M. Beresna, and P. G. Kazansky, "Dependence of the femtosecond laser refractive index change thresholds on the chemical composition of doped-silica glasses," Opt. Mater. Express **1**(4), 711–723 (2011).
5. J. B. Lonzaga, S. M. Avanesyan, S. C. Langford, and J. T. Dickinson, "Color center formation in soda-lime glass with femtosecond laser pulses," J. Appl. Phys. **94**(7), 4332–4340 (2003).
6. G. Lin, F. Luo, F. He, Q. Chen, D. Chen, Y. Cheng, L. Zhang, J. Qiu, and Q. Zhao, "Different refractive index change behavior in borosilicate glasses induced by 1 kHz and 250 kHz femtosecond lasers," Opt. Mater. Express **1**(4), 724–731 (2011).
7. H. Guillet de Chatellus and E. Freysz, "Characterization and dynamics of gratings induced in glasses by femtosecond pulses," Opt. Lett. **27**(13), 1165–1167 (2002).
8. G. D. Marshall, R. J. Williams, N. Jovanovic, M. J. Steel, and M. J. Withford, "Point-by-point written fiber-Bragg gratings and their application in complex grating designs," Opt. Express **18**(19), 19844–19859 (2010).
9. A. Martinez, M. Dubov, I. Khrushchev, and I. Bennion, "Direct writing of fibre Bragg gratings by femtosecond laser," Electron. Lett. **40**(19), 1170–1172 (2004).
10. S. J. Mihailov, C. W. Smelser, D. Grobnic, R. B. Walker, P. Lu, H. Ding, and J. Unruh, "Bragg gratings written in all-SiO_2 and ge-doped core fibers with 800-nm femtosecond radiation and a phase mask," J. Lightwave Technol. **22**(1), 94–100 (2004).
11. D. Grobnic, C. W. Smelser, S. J. Mihailov, R. B. Walker, and P. Lu, "Fiber Bragg gratings with suppressed cladding modes made in SMF-28 with a femtosecond IR laser and a phase mask," IEEE Photon. Technol. Lett. **16**(8), 1864–1866 (2004).
12. S. J. Mihailov, D. Grobnic, C. W. Smelser, P. Lu, R. B. Walker, and H. Ding, "Bragg grating inscription in various optical fibers with femtosecond infrared lasers and a phase mask," Opt. Mater. Express **1**(4), 754–765 (2011).
13. Ch. Voigtländer, R. G. Becker, J. Thomas, D. Richter, A. Singh, A. Tünnermann, and S. Nolte, "Ultrashort pulse inscription of tailored fiber Bragg gratings with a phase mask and a deformed wavefront," Opt. Mater. Express **1**(4), 633–642 (2011).
14. M. Bernier, S. Gagnon, and R. Vallée, "Role of the 1D optical filamentation process in the writing of first order fiber Bragg gratings with femtosecond pulses at 800nm," Opt. Mater. Express **1**(5), 832–844 (2011).

#175980 - $15.00 USD Received 11 Sep 2012; revised 22 Oct 2012; accepted 6 Nov 2012; published 8 Nov 2012

15. M. Ghanassi, M. C. Schanne-Klein, F. Hache, A. I. Ekimov, D. Ricard, and C. Flytzanis, "Time-resolved measurements of carrier recombination in experimental seconductor-doped glasses: confirmation of the role of Auger recombination," Appl. Phys. Lett. **62**(1), 78–80 (1993).
16. H. Kogelnik, "Coupled wave theory for thick hologram gratings," Bell Syst. Tech. J. **48**, 2909–2948 (1969).

1. Introduction

Nowadays, femtosecond laser pulses are largely used to induce permanent index modulations inside bulk glass [1,2]. These methods rely on the use of multiphoton absorption for the ultra-short release of the laser energy into such transparent material. This makes it possible to photo-write isotropic or non-isotropic three dimensional structures inside bulk glass [3]. Different studies have shown that such femtosecond irradiations induce structural changes of the glass that modify, on the sub-micrometric scale, the index of refraction [4]. The interaction of ultrafast laser pulses with soda-lime glasses and borosilicate glasses is also known for producing nonlinear effects including coloration. The latter also induces a change of the refractive index that is due to laser-induced color centers [5,6]. Hereafter, we have studied the impact of femtosecond laser-induced defects in a SF59 lead glass sample during the formation of photo-induced gratings. The grating is directly written into this glass sample by imaging a master grating, that is illuminated by the femtosecond laser pulses. With this technique it is possible to write directly a photo-induced grating [7]. The number of grooves per millimeter can be easily varied by changing the magnification of the optical device that images the master grating. Therefore, this technique offers many advantages compared to the direct write method [8,9] and the side-illumination with a phase mask [10–14]. Moreover, it is also possible to record the evolution of the grating during the writing process. Hereafter we apply this technique to demonstrate that the formation of the photo-induced grating has a non-instantaneous contribution that can be easily recorded on the microsecond time scale and that results from laser-induced defects. These defects impact both the real and the imaginary part of the index of refraction of the glass. Their contributions to the diffraction grating efficiency are evaluated. Under our experimental conditions, it is mainly the real part of the index of refraction that contributes to reflectivity the grating.

2. The experimental set-up

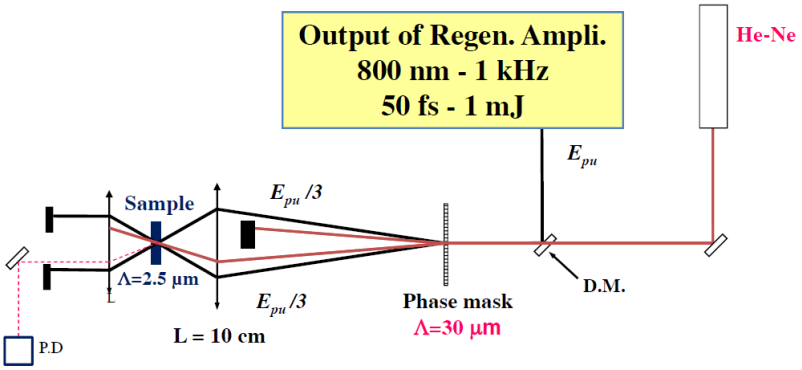

Fig. 1. The experimental set-up. D.M. stands for dichroic mirror.

To study the temporal evolution of gratings photo-induced by femtosecond laser pulses in glass, we used the experimental set-up sketched in Fig. 1. It has been previously described [7]. In short, a femtosecond pump beam delivered by a regenerative amplifier (1 mJ, ~50 fs, 1 kHz, ~800 nm) is used to photo-induce the grating. The pump-pulse is spatially overlapped with a continuous wave (CW) He-Ne laser beam that is used as a probe beam. Both beams are incident on a master phase-grating (spatial step L_1 = 30 µm) that is optimized to diffract ~65% of the intensity at 800 nm along + 1 and −1 diffraction orders. These two latter diffraction orders, that have almost the same intensity, are focused by a 100 mm focal-length lens to a

#175980 - $15.00 USD Received 11 Sep 2012; revised 22 Oct 2012; accepted 6 Nov 2012; published 8 Nov 2012

beam spot of ~180 µm in a 2 mm thick SF59 glass plate. Only the + 1 diffraction order of the He-Ne beam was focused on the sample. The direction of the diffracted He-Ne beam is along the −1 diffraction order of the grating. The intensity of the He-Ne beam diffracted by the photo-induced grating (spatial step L_2 = 2.5 µm.) is focused on a fast photodiode that has a rising time of ~1 ns and that is either connected to a lock-in amplifier or a 10 GHz sampling oscilloscope. The latter devices are used to record the intensity reflected by the grating on the second and the millisecond time-scale respectively. The 10 GHz sampling oscilloscope has 1 GHz bandwidth. The pump and probe beam were chopped independently.

3. Results

3.1 The grating formation

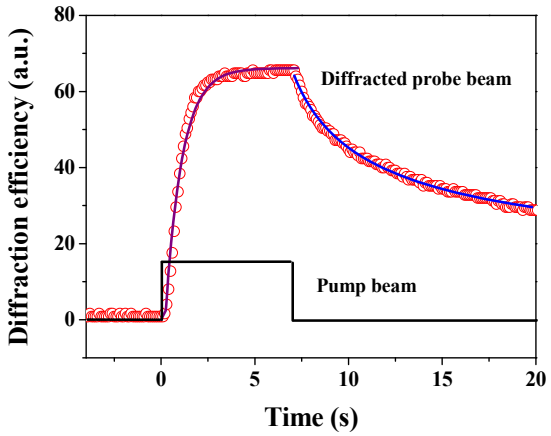

Fig. 2. Formation and relaxation of grating induced in SF59 for a peak power density of ~245 GW.cm^{-2}. The fits of the grating formation and relaxation are presented in solid lines. They are fitted by the equations $R(t) = R_0[1-\exp(-t/t)]$ and $R(t) = R_0(1/(At-B))$ respectively.

The typical evolution of the intensity of the He-Ne diffracted beam when the pump beam is on and off, or in other words during the formation and relaxation of the photo-induced grating, is presented in Fig. 2. When the pump beam is sent though the sample, one can readily record an increase of the intensity of the He-Ne diffracted beam. After a few seconds, the intensity saturates and reaches its steady state. The increase of the intensity of the diffracted beam is related to the increase of the density of defects photo-induced by the two-photon absorption of the sample at 800 nm. The higher the intensity of the pump beam, the higher the density of defects and the higher the reflectivity of the sample. When the pump beam is blocked, the photo-induced defects relax and the intensity of the diffracted beam decreases. The saturation intensity of the diffracted beam depends on both the pump power density and the exposure time of the sample to the pump beam. The impact of the exposure time for a given pump power of ~245 GW.cm^{-2} is presented in Fig. 3(a). As the exposure time increases, one clearly notices that the intensity of the diffracted beam increases and then reaches a saturation level. This saturation level depends on the pump peak power density. On the other hand, the time t_{sat} needed to reach the saturation level strongly depends on the pump peak power density: the lower the pump peak power, the longer t_{sat} (Fig. 3(b)) and the smaller the reflectivity of the grating. We will see that this latter evolution is related to the dynamics of the photo-induced defects.

#175980 - $15.00 USD Received 11 Sep 2012; revised 22 Oct 2012; accepted 6 Nov 2012; published 8 Nov 2012

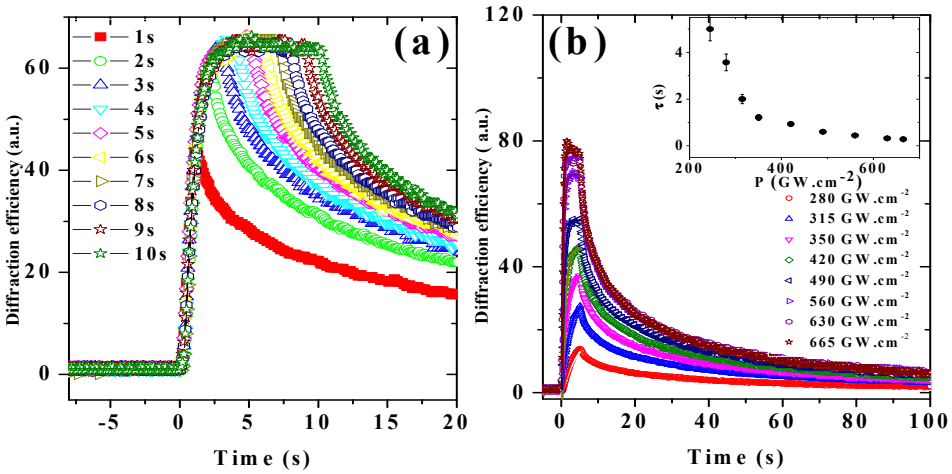

Fig. 3. (a) Formation and relaxation of a grating induced in SF59 versus the exposure time for a peak power density of ~245 GW.cm^{-2}. (b) Evolution of the grating formation and relaxation versus the pump power density P for a 5 s exposure time. The inset presents the evolution of characteristic time t versus the pump power density. The characteristic time t has been computed considering the grating reflectivity evolves according to the equations R(t) = R_0[1-exp(-t/t)]. The results of our fits are presented in solid lines.

3.2 Relaxation of the grating

Below the glass damage threshold, when the pump beam is blocked the intensity of the diffracted beam decreases down to zero (see Fig. 2). Note that the measured decay is non-exponential. This indicates that the grating is not induced by a thermal grating. Indeed, the multiphoton absorption of the pump pulse is expected to induce a thermal grating that should decay exponentially on the µs time scale. In practice, the reflectivity of such a grating is very weak and therefore it is not recorded by our set-up. However in agreement with our previous work we found the measured decay is well fitted by Auger recombination processes [7]. The decay of the grating when the irradiation is stopped is due to the relaxation of the photo-induced defect from N_0 to zero, where N_0 is the defect density just after excitation. The relaxation of the local density defects N(t) is well fitted by the following differential equation:

$$\frac{dN}{dt} = -AN - CN^3. \qquad (1)$$

The terms on the right-hand side of this equation correspond to classic exponential and Auger recombinations, respectively. It has been previously shown in the case of a dominant Auger recombination, N evolves as $\frac{1}{N^2} = \frac{1}{N_0^2} + 2Ct$ [7,15]. As the diffracted intensity is proportional to N^2, this is consistent with the experimental 1/t relaxation. The decay constant time C depends on the exposure time T and the pump power density P. For high pump power density or long exposure time, we noticed the reflectivity of the grating does not relax to zero indicating the presence of a permanent photo-induced grating. The ensemble of data agrees well with our previous work [7] but it does not reveal the evolution on time scale shorter than a second. Hence to investigate the evolution of the grating in more detail, we have carried out a detailed study of evolution of the grating on the millisecond time-scale.

3.3 Evolution of the grating in the transient and the steady state regime

Figure 4 presents the evolution of the diffracted intensity on the ten millisecond time-scales when the sample is excited by a sequence of pump pulses with different power density. One

#175980 - $15.00 USD Received 11 Sep 2012; revised 22 Oct 2012; accepted 6 Nov 2012; published 8 Nov 2012

should notice that the increase of the reflectivity is not instantaneous indicating that the grating continues to evolve in between two subsequent femtosecond pulses. The overall increase of the diffracted intensity depends on pump power density (Fig. 4(a)) but also on the number of pump pulses exciting the sample. In general, as one increases the number of exciting pulses, one records an increase of the overall diffraction efficiency. As presented in Fig. 4(b), we can also notice the occurrence of a steady state regime, where in between two successive exciting pulses, we first record an increase of diffracted intensity that relaxes back towards its initial value.

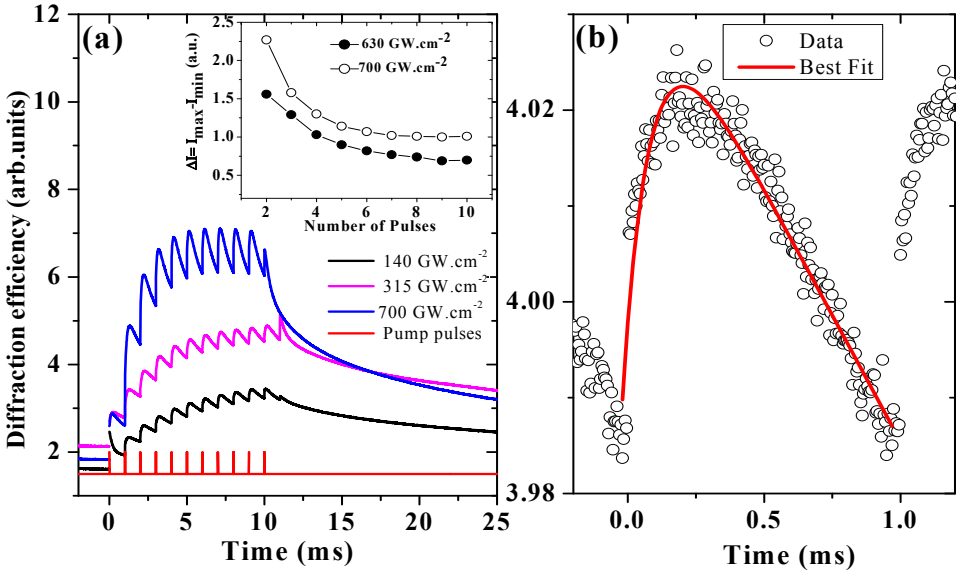

Fig. 4. (a) Evolution of the intensity diffracted He-Ne beam at millisecond time scale for 140, 315 and 700 GW.cm^{-2} pump peak power density. The inset presents the evolution of diffraction efficiency versus the order of pulses within the exciting pump pulse train for peak power density of 600 and 700 GW.cm^{-2} respectively. (b) (○) Evolution of the diffracted intensity recorded at steady state during pump pulse excitation. The femtosecond pump pulses are applied at t = 0 and t = 1 ms. (——): Fit of this data using the equation $R(t) = R_0\left[1-\exp\left(-\frac{t}{\tau}\right)\right]\left[\frac{1}{At-B}\right]$

Figure 4 presents the evolution of the grating on the millisecond time-scale when the steady state regime presented in Fig. 1 is reached. On this time-scale, our data were fitted using the following equation:

$$R(t) = R_0\left[1-\exp\left(-\frac{t}{\tau}\right)\right]\left[\frac{1}{At-B}\right]. \quad (2)$$

This equation accounts for both the formation and the relaxation of the grating. We have studied in more detail the evolution of the characteristic time constant (t, A^{-1}). These parameters account for the temporal increase and decrease of the reflectivity of the grating respectively. We found that the characteristic time t is almost independent of the number of pump pulses used to excite the sample whereas the characteristic time constant A^{-1} can strongly change between two subsequent exciting pump pulses. These latter results are presented in Fig. 5. This figure also indicates that A decreases and then saturates as the number of exciting pulses increases. Finally we stress that the value of characteristic time A^{-1} for the last exciting pulse agreed well with that found for the relaxation of the grating when

#175980 - $15.00 USD Received 11 Sep 2012; revised 22 Oct 2012; accepted 6 Nov 2012; published 8 Nov 2012

the pump beam was off. For instance in Fig. 5(a), for a power density of 245 GW.cm^{-2} and after exposure of the sample to 10 exciting pulses, the relaxation parameter is A = 7x10^{-10} s^{-1}, whereas for the same pump pulse peak, when the pump beam is stopped after 11 exciting pulses this relaxation parameter is A = 6.7x10^{-10} s^{-1}.

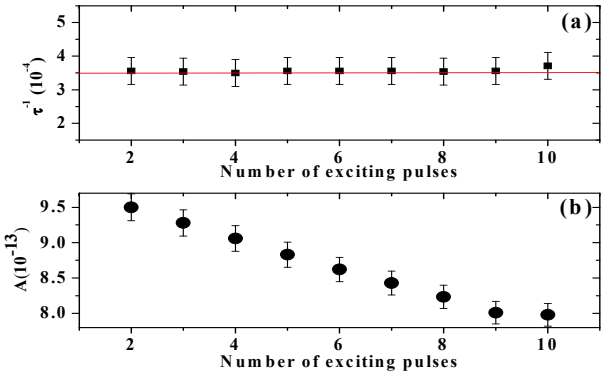

Fig. 5. (a) Evolution of the constant time t versus the number of exciting pulses. (b) Evolution of the constant time A^{-1} versus the number of exciting pulses. The data have been recorded for a pump peak power density of 245 GW.cm^{-2}.

These latter results make it possible to account for the saturation of the grating reflectivity presented in Fig. 3. As we previously mentioned, when the pump intensity increases, the number of defects induced increases as well. We therefore expect an increase of grating reflectivity with the pump intensity. Moreover, when the number of pulses that excites the sample increases, the number of defects also increases. While these two parameters result in an increase of the grating reflectivity, they also result in a decrease of the relaxation constant A. As a consequence, the photo-induced grating relaxes more and more rapidly as its reflectivity increases. Hence, in agreement with Fig. 3, the photo-induced grating reaches a saturation regime in which the increase of the grating reflectivity, induced by two successive exciting pulses, is compensated by the relaxation of the grating between these two exciting pulses.

3.4 Measurement of the photo-induced index variations at the steady state regime

While the previous measurements indicate that femtosecond lasers pulses make it possible to photo-induce transient or permanent gratings in lead doped glass, it does not indicate the origin or the amplitude of the modulations of the refractive index. With this goal in mind and using a very simple set-up, we have recorded the evolution of the real and the imaginary parts of refractive index (respectively, n_r, n_i) at the He-Ne laser wavelength (i.e. λ = 632.8 nm). The experiment was performed removing the master grating (see Fig. 1). The femtosecond beam was focused at normal incidence to a beam spot of ~180 µm. The He-Ne beam was parallel but spatially shifted with respect to the femtosecond beam. After the focusing lens and on the sample, it was more tightly focused (beam spot~140 µm) and slightly off normal incidence angle. The intensity of the transmitted He-Ne beam was detected by photodiode. The latter intensity is given by $I(e) = I_0 \exp\left(-4\frac{e\Delta n_i}{\lambda_{He-Ne}}\right)$ where I_0 is the transmitted intensity prior to femtosecond irradiation and e the sample thickness. It makes it possible to measure Dn_i. The He-Ne beams reflected by both the front and the back sides of the sample induce an interference pattern that can be recorded in the far field. By counting the fringe shift, one can easily deduce the variation of the real part of refractive index Dn_r induced by the femtosecond pump pulses. The relation between Dn_r and induced p-fringe shift is $Dn_r = p\, l_{He\text{-}Ne}/2e$. We could therefore easily calibrate the amplitude of Dn_r. To record Dn_r, the small sensitive area of the fast photodiode is placed on the maximum intensity of one of the bright fringes when the

#175980 - $15.00 USD Received 11 Sep 2012; revised 22 Oct 2012; accepted 6 Nov 2012; published 8 Nov 2012

pump beam is off. Figure 6 presents the evolution of the real and imaginary part of refractive index recorded at steady state versus the pump peak power density.

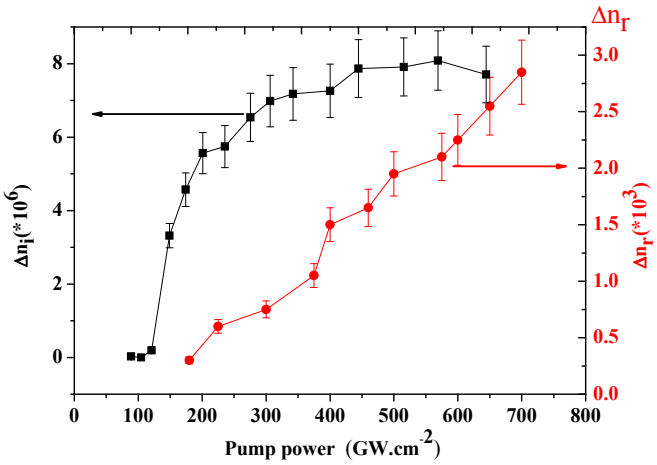

Fig. 6. Change of the real Dn_r and imaginary Dn_i part of the index of refraction in SF 59 glass with respect to the pump power density.

3.5 Kinetics of the photo-induced index variations

This set-up also makes it possible to record the evolution of the real and imaginary part of the index of refraction of the sample. These evolutions are presented in Fig. 7. When the pump beam is on, the absorption and the index of refraction of the sample increase. They relax when the pump beam is off. Recall that these latter coefficients are related by a Kramers-Kronig transformation.

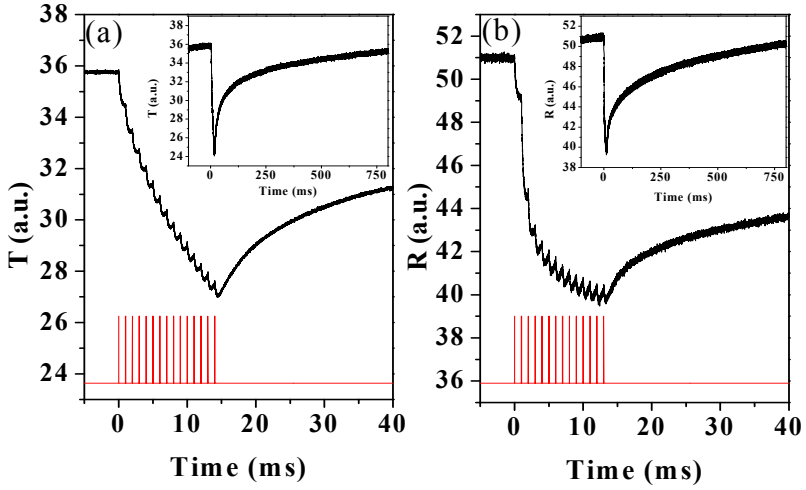

Fig. 7. Evolution of the real Dn_r (a) and imaginary Dn_i (b) part of the index of refraction in SF 59 glass. The insets present the evolution on a longer time scale.

The sign of Dn_r was inferred from the thermal index variation of the SF59 sample. In the latter case, we recorded the direction in which the fringes were shifted upon a temperature increase of the sample and compared it to the direction in which the fringes are shifted upon

#175980 - $15.00 USD Received 11 Sep 2012; revised 22 Oct 2012; accepted 6 Nov 2012; published 8 Nov 2012

femtosecond laser excitation. We found that both were moving in the same direction. Knowing $dn_r/dT \sim -5\ 10^{-7}\ K^{-1}$ for SF59, we concluded Dn_r was negative.

This ensemble of measurements makes it possible to evaluate the contributions of both the real and imaginary part of the grating diffraction efficiency. The general expression for the grating reflectivity is: $I(e) = I_0(\sin^2(\frac{\pi}{2\lambda}\Delta n_r\, e) + \sinh^2(\frac{\pi}{2\lambda}\Delta n_r e))\exp(-\frac{3\pi}{2\lambda}\Delta n_i e)$ [16]. In our experiments, the contribution of the imaginary part of the index of refraction to the grating diffraction efficiency is negligible: $\sin^2(\frac{\pi}{2\lambda}\Delta n_r\, e) >> \sinh^2(\frac{\pi}{2\lambda}\Delta n_r e)$, and hence $R(t) = \left[\sin^2(\frac{\pi}{2\lambda}\Delta n_r(t)\, e)\right]\exp(-\frac{3\pi}{2\lambda}\Delta n_i e)$. In other words, the reflectivity of our gratings is mainly due to the change of Dn_r but its amplitude is modulated by Dn_i. Finally, and in agreement with previous works [5,6], we show that the femtosecond excitation induces a broad absorption over the whole visible spectral range (Fig. 8). It is the latter that accounts for the different evolution recorded for Dn_r and Dn_i.

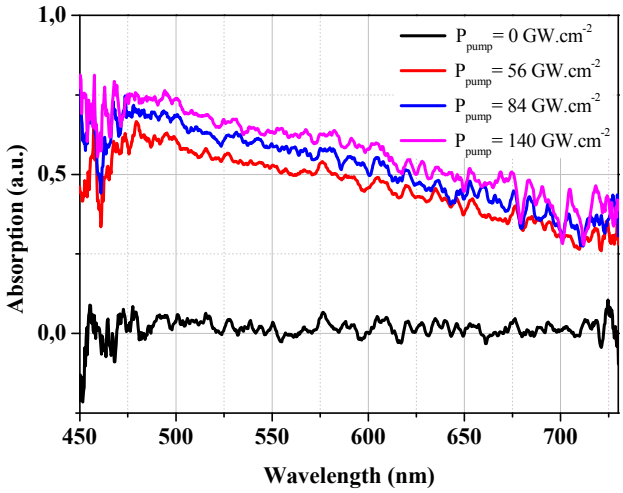

Fig. 8. Evolution of absorption spectrum of the SF 59 glass excited by different pump pulse peak power densities.

4. Discussion

Hereafter, we briefly discuss the origin of the photo-induced defects. The two photon absorption at 800 nm is well into the absorption edge of the SF59 glass. Hence sufficiently intense ultrafast laser pulses will produce a high density of electron-hole pairs. It was previously proposed that the trapping, detrapping and recombination of these excitation accounts for the behavior of the darkening and partial recovery on both slow and fast time scales [6,7]. In fact femtosecond laser irradiation, x rays and γ rays induced similar darkening in many different glasses. For instance it has been shown that the formation of hole centers (such as H_2^+ or OHC_1 centers and H_3^+or OHC_2 centers) induces absorption peaks in the visible spectral range. Similarly the production of electron traps (denoted E_3^- and E_4^- centers) results in an enhancement of the absorption in the near UV. Therefore, both defects could contribute to the index modification of our photo-excited sample. As previously shown, the partial bleaching or recovery of the sample is attributed to the electron-hole recombination that occurs between laser pulses [6].

#175980 - $15.00 USD Received 11 Sep 2012; revised 22 Oct 2012; accepted 6 Nov 2012; published 8 Nov 2012

5. Conclusion

We have investigated the interaction of ultrafast laser pulses with SF59 glass. Although this glass is not considered as photosensitive, the high peak power density of the used femtosecond pulses makes it possible to photo-induce transient or permanent gratings within this material. We have shown that the latter grating results from laser induced defects that induce a coloration of the glass on the whole visible spectral range. We have shown the defects are induced by a single femtosecond pulse but continue to increase on the millisecond timescale. Considering the optical properties of these gratings, it would be useful to characterize completely the index variation at smaller timescale. However this work presents promising results for the understanding of optical data storage in glasses.

Acknowledgments

The authors thank the Aquitaine Region for supporting this project with the development of the COLA Platform and the ANR Agency (FLAG-09-BLAN-495203).

#175980 - $15.00 USD Received 11 Sep 2012; revised 22 Oct 2012; accepted 6 Nov 2012; published 8 Nov 2012